Performic Acid Oxidation of 1-Methylbicyclo[2.2.1]hept-5-en-2-one. Elucidation of Reaction Products by Multinuclear NMR Spectroscopy, X-Ray Diffraction and Molecular Mechanics Calculations

Katri Laihia,* Kari Rissanen, Erkki Kolehmainen, Jorma Korvola and Kari Leskinen

Department of Chemistry, University of Jyväskylä, SF-40100 Jyväskylä, Finland

Laihia, K., Rissanen, K., Kolehmainen, E., Korvola, J. and Leskinen, K., 1991. Performic Acid Oxidation of 1-Methylbicyclo[2.2.1]hept-5-en-2-one. Elucidation of Reaction Products by Multinuclear NMR Spectroscopy, X-Ray Diffraction and Molecular Mechanics Calculations. – Acta Chem. Scand. 45: 499–507.

Structures of three stereochemically isomeric lactones, *endo,exo*-7,8-dihydroxy-*exo*-7-methyl- (**1**), *exo,endo*-7,8-dihydroxy-*endo*-7-methyl- (**2**) and *endo,endo*-7,8-dihydroxy-*exo*-7-methyl-2-oxa-*cis*-bicyclo[3.3.0]octan-3-one (**3**) have been elucidated by use of ^{1}H, ^{13}C, ^{17}O NMR, IR and mass spectroscopy, X-ray diffraction and molecular mechanics calculations. The lactones **1**, **2** and **3** are all Baeyer–Villiger performic acid oxidation products of 1-methylbicyclo[2.2.1]hept-5-en-2-one. ^{1}H and ^{13}C chemical shifts and vicinal $^{3}J_{H,H}$ coupling constants are in accordance with X-ray data, which show an *endo* conformation for **1** and an *exo* conformation for **2**. Molecular mechanics calculations were used to estimate the dihedral angles between vicinal protons and to calculate the corresponding $^{3}J_{H,H}$ coupling constants and especially to solve the third lactone structure in the absence of X-ray data. Lactone **1** crystallizes in an orthorhombic space group *Pbca* (No. 61) with cell dimensions: a 17.606(5), b = 9.760(3), c = 9.693(2) Å and V = 1666(1) Å^{-3} with Z = 8. Full-matrix least-squares refinement of 145 parameters gave R = 0.063 for 870 reflections [$I>1.5\sigma I$]. The O····C=O interaction between the *endo* oxygen O(7) and the carbonyl carbon C(3) is strong in lactone **1** with an intramolecular O····C=O distance of 2.851(6) Å. Lactone **2** crystallizes in a triclinic space group *P*-1 (No. 2) with cell dimensions: a = 5.976(1), b = 7.160(2), c = 10.307(2) Å, α = 83.43(1), β = 79.01(1), γ = 75.23(1)° and V = 417.6(1) Å^{-3} with Z = 2. Full-matrix least-squares refinement of 145 parameters gave R = 0.040 for 683 reflections [$I>1.5\sigma I$]. The O····C=O interaction between the *endo* oxygen O(8) and carbonyl carbon C(3) is not as evident as in lactone **1** and the intramolecular O····C=O distance is 3.265(4) Å.

Oxidation of bicyclo[2.2.1]hept-5-en-2-ones with organic peracids has been proved to occur solely with regioselective oxygen insertion and migration of the allylic bridgehead position. In these Baeyer–Villiger type reactions, the bridged, unsaturated bicyclic ketones can be converted into unsaturated, oxygen-inserted lactones, unsaturated rearranged lactones and their derivatives. The oxygen-insertion lactones have been much used as intermediates in the stereoselective synthesis of alkaloids, steroids, carbohydrates, prostaglandins and terpenoid natural products.[1-4]

This paper describes an oxidation of 1-methylbicyclo[2.2.1]hept-5-en-2-one (1-methyl-5-norbornen-2-one) with performic acid to give three isomeric dihydroxylactones, derivatives of 2-oxa-*cis*-bicyclo[3.3.0]octan-3-one.

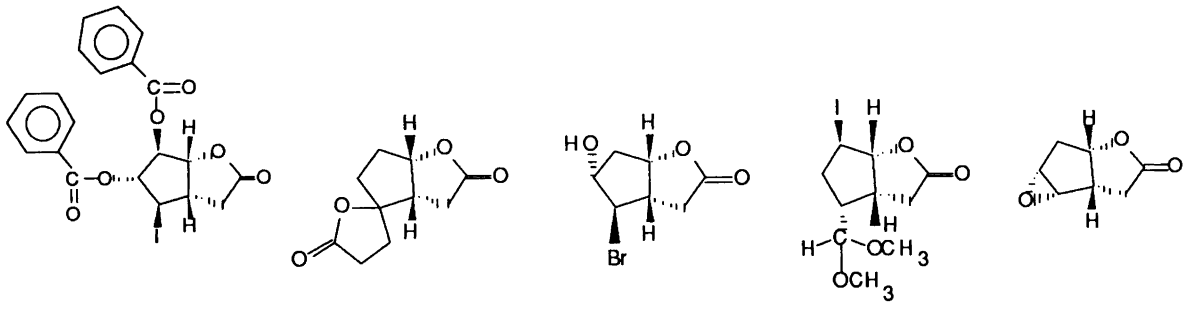

Fig. 1. **5** **6** **7** **8** **9**

* To whom correspondence should be addressed.

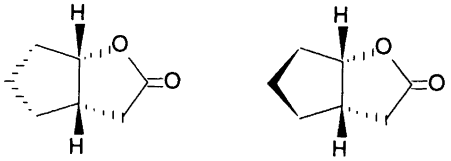

Scheme 1.

The reactions leading to these compounds include a regioselective Baeyer–Villiger oxygen-insertion reaction, rearrangement of the bicyclic lactone and oxidation of the carbon–carbon double bond.

Crystallographic studies on 2-oxa-*cis*-bicyclo[3.3.0]octan-3-one derivatives **5**,[2] **6**,[3] **7**,[4] **8**[5] and **9**[6] show that the bicyclic *cis* lactone moiety preferably adopts the *endo* conformation (Scheme 1). In addition intramolecular interaction between an *endo* oxygen (cyclopentane ring substituent) and the carbonyl carbon occurs especially in the *endo* conformation. This O····C=O interaction, which can be inter- or intra-molecular, has been defined by Bürgi *et al.*[7] and occurs between a nucleophile (oxygen or nitrogen) and an electrophile (carbonyl carbon) when they are in sterically favourable positions. The incipient nucleophilic attack of an oxygen atom on a carbonyl group involves O····C=O distances (*d*) of 2.7 Å (strong) to 3.1 Å (negligible) and the optimum O····C=O angle (α) of attack is ca. 105°. This interaction was also found to produce a small out-of-plane deformation (Δ) of the electrophilic carbonyl carbon towards the nucleophilic oxygen (Scheme 2).[7]

The strongest intramolecular O····C=O interaction of lactones **5**–**9** was found in lactone **9** where d = 2.992 Å, α 118.8° and Δ = 0.010(2) Å and lactone **7** with d = 2.998 Å, α = 113° and Δ = 0.010(2) Å, which have *endo* conformations, whereas in lactone **6** (*exo* conformation) the intermolecular distance is 3.335 Å, indicating negligible interaction.

The structures of the present reaction products could not be elucidated solely by means of NMR spectroscopy. The mutual interaction of the hydroxy oxygens and the lactone carbonyl group (O····C=O) as well as the interaction between the methyl and two hydroxy substituents disturb the bicyclic lactone skeleton in such a way that additional information from X-ray diffraction and molecular mechanics calculations was needed for an unambiguous structure assignment.

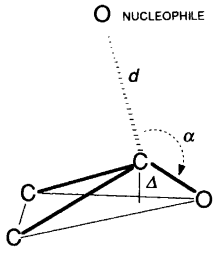

Scheme 2.

Experimental

Preparation of compounds **1**–**3**. The starting compound 1-methyl-5-norbornen-2-one was synthesized by a known method[8,9] and oxidized with performic acid using the reaction procedure described by Paasivirta and Äyräs.[10] The reaction mixture was separated using flash chromatography: 55 mm × 350 mm Kieselgel 60 (mesh 230–400) column and light petroleum (b.p. 40–60 °C)–acetone (7:5) as the eluent. The separation of coumpounds was followed by gas chromatography. The compounds obtained were recrystallized from ethanol. Melting points are: 151–154 (**1**), 164–167 (**2**) and 105–108 °C (**3**). IR spectra showed the following hydroxy and carbonyl group absorptions (cm^{-1}): 3395.3, 3302.8 and 1726.4 (**1**); 3379.1, 3200.0, 1741.4 and 1723.3 (**2**); 3325.0 and 1767.9 (**3**), respectively. The mass spectra for **1**–**3** cannot be used to identify the isomers. The main peaks and peaks heights (percentage in parentheses) in almost identical spectra are: 41 (42), 42 (21), 43 (100), 45 (10), 55 (24), 57 (16), 58 (45), 69 (36), 70 (12), 71 (27), 83

Table 1. Experimental crystallographic data for **1** and **2**.

Compound	**1**	**2**
Formula	$C_8H_{12}O_4$	$C_8H_{12}O_4$
m_r	172.18	172.18
a/Å	17.606(5)	5.976(1)
b/Å	9.760(3)	7.160(2)
c/Å	9.693(2)	10.307(2)
α/°	90	83.43(1)
β/°	90	79.01(1)
γ/°	90	75.23(1)
V/Å^3	1666(1)	417.6(2)
Z	8	2
d_{calc}/Mg m^{-3}	1.373	1.369
μ/mm^{-1}	0.10	0.10
λ/MoK_α	0.71073	0.71073
F(000)	736	184
Space group	*Pbca* (No. 61)	*P*-1 (No. 2)
T/K	296±1	296±1
Crystal size/mm	0.20×0.17×0.19	0.15×0.20×0.22
Refl. for latt. meas.	25	25
θ range for latt. meas./°	5–12	8–14
Scan method	ω/2θ	ω/2θ
Scan speed/° min^{-1}	1–17	1–17
Scan width (ω)/°	1.0 + 0.34 tanθ	1.0 + 0.34 tanθ
θ range/ °	2–25	2–20
h range	0 → 20	0 → 5
k range	0 → 11	−6 → 6
l range	0 → 11	−9 → 9
Variation of std. refl.	None	None
Refl. measured	1724	777
No. of unique refl.	1724	777
Condition of obs. refl.	$I > 1.5\sigma(I)$	$I > 1.5\sigma(I)$
Refl. used in refinement	870	683
Max. shift/error	0.02	<0.01
No. of param.	145	145
Max./min. in final Δϱ/e Å^{-3}	0.27(7)/−0.20(7)	0.14(4)/−0.15(4)
S	1.11	1.64
R	0.063	0.040
R_w	0.061	0.039
$w = 1/[(\sigma F_o)^2 + (a F_o)^2]$	a = 0.01	a = 0.003

(20), 84 (58), 95 (21), 97 (26), 98 (12), 109 (11), 111 (28), 112 (14), 113 (11), 126 (43), 139 (4) and 154 (6).

Crystal structure analysis of **1** *and* **2**. The crystal data and conditions for the data collections are given in Table 1.* The lattice parameters were determined measuring 25 reflections using Mo K_α (λ = 0.71073 Å) radiation at room temperature (296 K). Intensity data were collected on an Enraf-Nonius CAD4 diffractometer. The intensity data were corrected for Lorentz and polarization effects but not for extinction. Empirical absorption correction was carried out according to Walker and Stuart[11] for both data sets, the maximum and minimum correction coefficients being 1.135 and 0.928 for **1** and 1.201 and 0.678 for **2**, respectively. The structure was solved by direct methods using the MULTAN11/82 program.[12] The final refinements were carried out by full matrix least-squares calculations using the SDP-plus program package,[13] anisotropically for all non H-atoms. The hydrogen atoms were located from ΔF calculations and refined isotropically with fixed isotropic temperature factor (B = 5.0 Å^2). The atomic scattering factors were taken from Ref. 14. The final coordinates are given in Tables 2 and 3. In addition to the programs quoted, the PLUTO[15] program was used. The crystallographic calculations were performed on a μ-VAX II computer at the Department of Chemistry, University of Jyväskylä.

Table 2. Fractional coordinates and equivalent isotropic temperature factors[a] for **1**.

Atom	x	y	z	B_{eq}/Å^2
O(2)	0.2915(2)	−0.0615(3)	0.9243(3)	3.04(7)
O(3)	0.3447(2)	−0.1932(4)	1.0822(3)	4.21(8)
O(7)	0.3992(2)	0.1422(3)	1.0103(3)	2.68(6)
O(8)	0.2978(2)	0.2331(3)	0.6950(3)	3.01(7)
C(1)	0.3122(3)	0.0110(4)	0.7981(5)	2.5(1)
C(3)	0.3504(3)	−0.1338(5)	0.9728(5)	3.1(1)
C(4)	0.4146(3)	−0.1382(5)	0.8721(5)	3.0(1)
C(5)	0.3954(3)	−0.0271(4)	0.7656(4)	2.6(1)
C(6)	0.4407(3)	0.1069(5)	0.7816(4)	2.5(1)
C(7)	0.3904(3)	0.1975(5)	0.8730(4)	2.4(1)
C(8)	0.3102(3)	0.1637(4)	0.8242(4)	2.4(1)
C(9)	0.4116(3)	0.3489(5)	0.8726(5)	3.6(1)
H(1)	0.266(3)	−0.018(5)	0.724(7)	5.0
H(4B)	0.468(3)	−0.116(6)	0.918(6)	5.0
H(4A)	0.422(3)	−0.239(5)	0.828(6)	5.0
H(5)	0.401(3)	−0.066(5)	0.673(6)	5.0
H(6B)	0.492(3)	0.080(5)	0.838(6)	5.0
H(6A)	0.445(3)	0.157(5)	0.709(6)	5.0
H(O7)	0.358(3)	0.169(5)	1.064(6)	5.0
H(O8)	0.252(3)	0.217(6)	0.669(6)	5.0
H(8)	0.266(3)	0.191(6)	0.900(6)	5.0
H(9B)	0.402(3)	0.397(6)	0.784(6)	5.0
H(9C)	0.377(3)	0.395(6)	0.928(6)	5.0
H(9A)	0.465(3)	0.358(6)	0.901(6)	5.0

[a] $B_{eq} = (4/3)\Sigma_i\Sigma_j\beta_{ij}\boldsymbol{a}_i \cdot \boldsymbol{a}_j$.

* Lists of structure factors, anisotropic temperature factors and least-squares planes may be obtained from one of the authors (K.R.) on request.

Table 3. Fractional coordinates and equivalent isotropic temperature factors[a] for **2**.

Atom	x	y	z	B_{eq}/Å^2
O(2)	−0.0305(3)	0.6836(3)	0.5833(2)	4.40(5)
O(3)	−0.2915(4)	0.9600(3)	0.6169(3)	5.89(7)
O(7)	0.5891(3)	0.3346(3)	0.6990(2)	3.75(5)
O(8)	−0.0423(3)	0.4227(3)	0.7960(2)	5.02(6)
C(1)	0.1914(5)	0.5789(4)	0.6190(3)	3.25(7)
C(3)	−0.1104(5)	0.8511(4)	0.6395(3)	3.93(8)
C(4)	0.0511(6)	0.8784(4)	0.7236(4)	5.7(1)
C(5)	0.2659(5)	0.7111(4)	0.7030(3)	3.97(8)
C(6)	0.3335(5)	0.5847(5)	0.8254(3)	4.05(8)
C(7)	0.3674(5)	0.3786(4)	0.7891(3)	3.26(7)
C(8)	0.1770(5)	0.3951(4)	0.7059(3)	3.31(7)
C(9)	0.3695(6)	0.2276(5)	0.9038(3)	5.4(1)
H(1)	0.301(6)	0.549(5)	0.537(3)	5.0
H(4B)	−0.029(6)	0.873(4)	0.815(3)	5.0
H(4A)	0.069(6)	1.006(5)	0.699(3)	5.0
H(5)	0.392(6)	0.754(5)	0.653(3)	5.0
H(6A)	0.478(5)	0.599(4)	0.852(3)	5.0
H(6B)	0.193(6)	0.606(5)	0.905(3)	5.0
H(O7)	0.633(5)	0.199(5)	0.679(3)	5.0
H(O8)	−0.138(6)	0.396(4)	0.747(3)	5.0
H(8)	0.215(5)	0.276(5)	0.650(3)	5.0
H(9A)	0.220(5)	0.264(5)	0.964(3)	5.0
H(9B)	0.516(5)	0.217(4)	0.947(3)	5.0
H(9C)	0.388(6)	0.095(5)	0.876(3)	5.0

[a] $B_{eq} = (4/3)\Sigma_i\Sigma_j\beta_{ij}\boldsymbol{a}_i \cdot \boldsymbol{a}_j$.

NMR, IR and mass spectra and molcular mechanics calculations. The ^{1}H and ^{13}C NMR spectra were recorded with a JEOL GSX 270 MHz FT NMR spectrometer at 30 °C for 0.2–0.5 M solutions in pyridine-d_5. In all ^{1}H measurements the digital resolution was 0.11–0.07 Hz, the number of scans was 4 and the flip angle 90°. In ^{13}C measurements, the digital resolution for all proton-noise-decoupled ^{13}C spectra was 1.0 Hz and the number of scans was 200–800. For fully coupled spectra the digital resolution was 0.31 Hz and the number of scans 13000–35000. The ^{17}O NMR proton-noise-decoupled spectra were measured at 36.50 MHz with a JEOL GSX 270 MHz FT NMR spectrometer for 0.12 M (**1** and **2**) and 0.02 M (**3**) solutions in acetone-d_6. The spectral settings were: spectral width 36 kHz, number of data points 8000, number of scans 200 000–300 000 at 40 °C, acquisition time 0.06 s and pulse delay 0.3 s. The ^{17}O chemical shifts were referenced to the signal of external D_2O in a capillary tube inserted coaxially into the NMR tube. To improve the S/N ratio in the frequency spectra all FIDs were windowed by a factor of the digital resolution (exponential line broadening of 100 Hz for ^{17}O) before Fourier transformation. The proton and carbon chemical shifts were also assigned from their HH-COSY and CH-COSY spectra. The chemical shifts are referenced to the internal tetramethylsilane. IR spectra were recorded with a Perkin–Elmer 283 spectrometer as KBr wafers (1:200 mg). The mass spectra were recorded with a Varian MAT 212 at 70 eV. The second-order ^{1}H NMR spectra were analysed by means of an iterative, modified LAOCOON-type program MAOCON[16] using a VAX 8650 computer at the Computer

Center of the University of Jyväskylä. Molecular mechanics calculations were performed using the program PCMODEL[17] (Serena Software) with default force constants on a Hewlett–Packard Vectra QS/16S personal computer.

Results and discussion

The peroxidation of 1-methyl-5-norbornen-2-one (**i**) gave three isomeric lactones, which are presented in Fig. 2. The possible reaction mechanisms leading to these structures are presented in Scheme 3. The reaction starts with a regioselective oxygen insertion and rearrangement of the intermediate lactone **II** to carbocations **IIIa** and **IIIb**. These probably give the unsaturated lactone **IV** as an intermediate; however, this could not be isolated. Lactone **IV** can then continue the reaction through the epoxylactones **V** and **VI**, or the carbocations **VII** and **VIII** can be the subsequent intermediates. As can be seen in Scheme 3, both epoxylactones (**V** and **VI**) will give the lactones **1** and **2** as final reaction products. Carbocation **VII** leads to lactones **2** and **3**, whereas carbocation **VIII** would give the lactones **1** and **4**. Compound **4**, however, was not found among the reaction products.

The ^{1}H and ^{13}C chemical shifts and $^{1}J_{C,H}$ coupling constants for the lactones **1–3** are presented in Tables 4 and 5. The observed vicinal, $^{3}J_{H,H}$, coupling constants are in agreement with structure **1**. The experimental dihedral angles from a crystal structure study of **1** are consistent with the $^{3}J_{H,H}$ coupling constants calculated by means of the well known, refined Karplus-type relationship.[18]

In the ^{1}H NMR spectra for lactones **2** and **3** the $^{3}J_{H,H}$ values for H(1) and H(8), 3.6 (**2**) and 4.7 Hz (**3**), respectively, suggest that O(8) is situated on the opposite side of the cyclopentane ring relative to H(1). However, the large coupling between H(4B) and H(5) in **2** (7.3 Hz), as well as the large couplings between H(5) and H(6B) (6.5 Hz in **2** and 8.5 Hz in **3**), were not appropriate for the expected structures. In lactone **1** these coupling constants were clearly smaller than those between H(4A) and H(5) and between H(5) and H(6B), where the experimental dihedral angles are close to 100°. The crystal structure study for lactone **2** revealed an *exo* conformation for the bicyclic lactone skeleton, where the observed vicinal coupling constants, $^{3}J_{H,H}$, are in accordance with the experimental dihedral angles (Tables 6 and 8). The dihedral angles H(4B)–C(4)–C(5)–H(5) and H(5)–C(5)–C(6)–H(6B) in **2** are −136 (3) and 146(3)°, respectively.

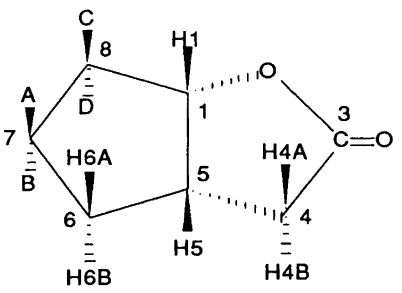

Lactone **1**, A = CH_3, B = OH, C = OH and D = H
Lactone **2**, A = OH, B = CH_3, C = H and D = OH
Lactone **3**, A = CH_3, B = OH, C = H and D = OH

Fig. 2. The structures and numbering of lactones **1**, **2** and **3**.

Table 4. ^{1}H Chemical shifts in ppm and $^{n}J_{H,H}$ (n = 2–4) in Hz for **1–3**.

Proton	δ(ppm)		
	1	**2**	**3**
H(1)	5.12	5.54	5.16
H(4A)	2.83	2.81	2.79
H(4B)	2.74	2.54	2.37
H(5)	3.09	3.15	3.23
H(6A)	2.37	2.31	1.53
H(6B)	1.92	1.99	2.33
H(8)	4.46	4.28	4.12
CH_3	1.47	1.65	1.46
Coupling	$^{n}J_{H,H}$/Hz		
	1	**2**	**3**
1,5	8.5	9.0	8.8
1,8	—	3.6	4.7
4A,4B	−18.1	−18.0	−18.4
4A,5	11.7	11.5	10.7
4B,5	3.9	7.3	3.9
5,6A	8.9	9.0	9.8
5,6B	1.8	6.5	8.5
6A,6B	−13.3	−13.2	−13.4
6B,8	1.5	—	—

Table 5. ^{13}C Chemical shifts in ppm and $^{1}J_{C,H}$ in Hz for **1–3**.

Carbon	**1**		**2**		**3**	
	δ(ppm)	$^{1}J_{C,H}$/Hz	δ(ppm)	$^{1}J_{C,H}$/Hz	δ(ppm)	$^{1}J_{C,H}$/Hz
C(1)	91.5	157.3	86.5	157.6	91.7	158.0
C(3)	176.8	—	179.2	—	178.0	—
C(4)	37.3	133.0	37.4	134.0	35.4	132.5
C(5)	35.7	135.2	35.5	136.4	34.0	139.8
C(6)	45.0	130.3	45.6	129.9	44.3	129.2
C(7)	81.0	—	81.3	—	78.1	—
C(8)	82.4	146.5	78.1	149.2	83.9	139.9
C(9)	23.2	125.5	23.4	125.0	24.7	125.2

The ^{17}O NMR spectra for the lactones **1–3** were measured to verify the proposed structures. The ^{17}O chemical shifts are presented in Table 7. The most significant differences are in the values of the chemical shift of the ethereal oxygen (–O–). The ^{17}O chemical shift of the lactone oxygen in **2** is 188.4 ppm, whereas the corresponding values in **1** and **3** are 201.2 and 198 ppm, respectively. These values are in agreement with the similar spatial substitution in C(7) for **1** and **3** with intramolecular O···C=O interaction. Al-

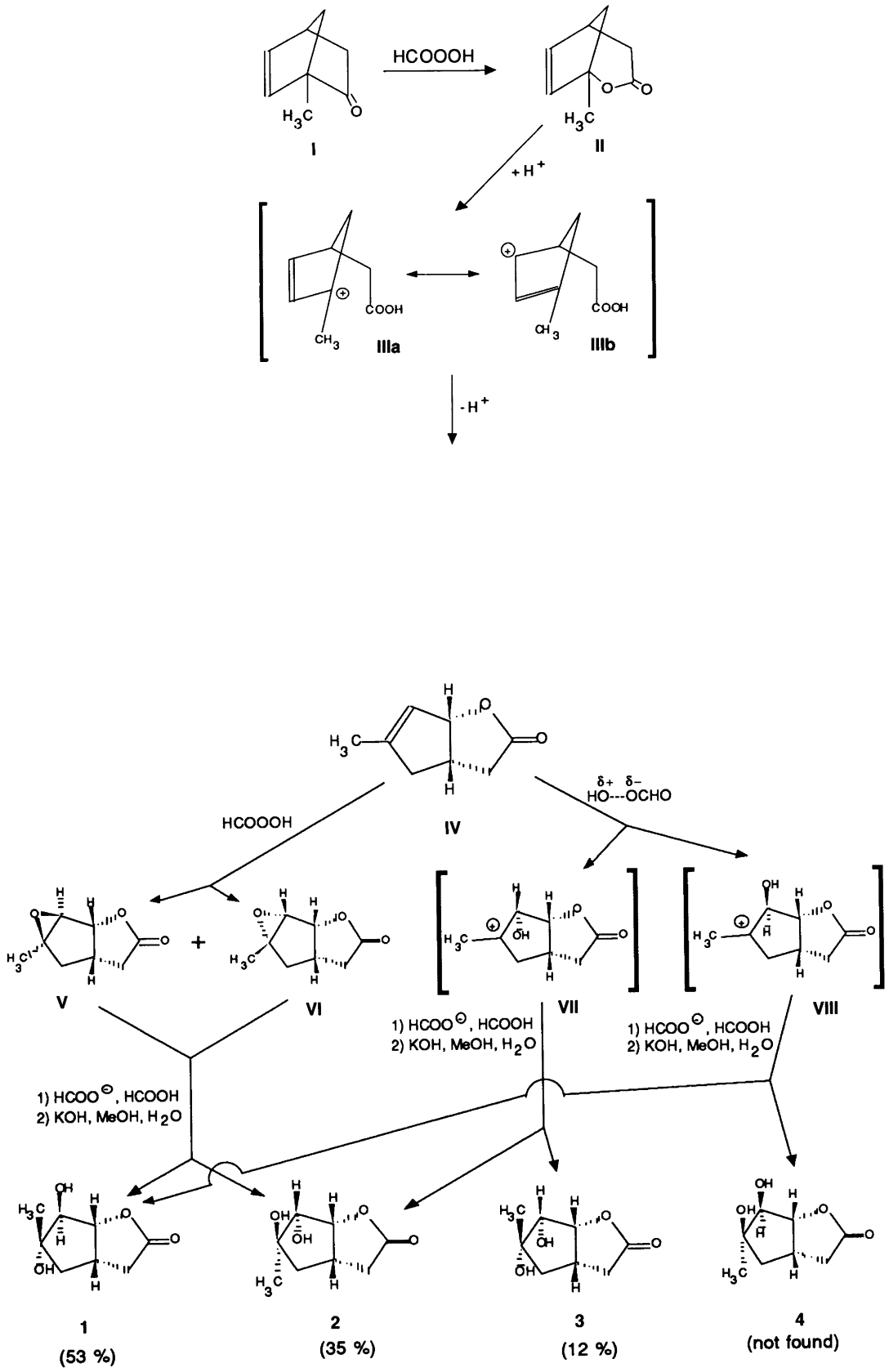
HCOOOH
I
II
+H+
IIIa
IIIb
-H+
IV
δ+ δ−
HO---OCHO
HCOOOH
V
VI
VII
VIII
1) HCOO⊖, HCOOH
2) KOH, MeOH, H2O
1) HCOO⊖, HCOOH
2) KOH, MeOH, H2O
1) HCOO⊖, HCOOH
2) KOH, MeOH, H2O
1
(53 %)
2
(35 %)
3
(12 %)
4
(not found)

Scheme 3.

Table 6. [a]Experimental and *calculated* dihedral angles (°) and corresponding $^3J_{H,H}$/Hz.

Lactone		Dihedral angle/H–C–C–H					
		1–1–5–5	1–1–8–8	4A–4–5–5	4B–4–5–5	5–5–6–6A	5–5–6–6B
1	X-Ray/°	7(5)	80(5)	−9(5)	107(5)	32(5)	−101(5)
	$^3J_{H,H}$/Hz	8.1	0.7	11.8	3.9	8.9	1.8
	MMX/°	*9*	*85*	*10*	*111*	*24*	*94*
	$^3J_{H,H}$/Hz	*8.4*	*0.7*	*10.0*	*3.1*	*8.5*	*1.2*
2	X-Ray/°	8(3)	−27(3)	−10(3)	−136(3)	19(3)	146(3)
	$^3J_{H,H}$/Hz	9.0	3.6	11.5	7.3	9.0	6.5
	MMX/°	*11*	*34*	*14*	*137*	*15*	*135*
	$^3J_{H,H}$/Hz	*9.3*	*5.0*	*9.8*	*7.5*	*9.7*	*7.2*
3	X-Ray/°	—	—	—	—	—	—
	$^3J_{H,H}$/Hz	8.8	4.7	10.7	3.9	9.8	8.5
	MMX/°	*5*	*31*	*8*	*131*	*20*	*140*
	$^3J_{H,H}$/Hz	*9.3*	*5.3*	*10.2*	*6.3*	*9.2*	*8.1*

[a]MMXE *optimized minimum energies* in kcal mol^{-1}: **1** = *16.70*, **2** = *16.91* and **3** = *17.72*.

though the interpretation of the present ^{17}O NMR data is not straightforward, the remarkable differences between stereoisomers in their ^{17}O NMR chemical shifts suggest that ^{17}O NMR spectroscopy could be useful in the structure elucidation of compounds possessing the lactone moiety when suitable model compounds are available.

Molecular mechanics (MMX) were also used to estimate the energetically most preferred structures for the lactones formed. Molecular mechanics optimizations gave the structures directly, which are in agreement with X-ray and NMR data in the case of lactones **1** and **2**. The calculated minimum energy for the lactone **2**, 16.91 kcal mol^{-1}, is quite close to that obtained for the main reaction product, lactone **1** (16.70 kcal mol^{-1}). As can be seen from Table 6, the experimental (X-ray) and calculated (MMX) dihedral angles and the corresponding experimental and calculated $^3J_{H,H}$ values are very close to each other. Lactone **3** did not give crystals suitable for study by X-ray diffraction. Therefore molecular mechanics calculations in connection with ^1H NMR data for **1–3** and experimental dihedral angles for **1** and **2** were used to assign a structure for lactone **3**.

First the structures for both **3** and **4** were optimized by energy minimization. The calculated minimum energy was 0.41 kcal mol^{-1} smaller for lactone **4**. However, the calculations always gave two small vicinal coupling constants ($^3J_{H,H}$ = 1.5 and 0.7 Hz) for the structure **4**, which deviate remarkably from the corresponding observed values. Thus structure **4** was rejected and structure **3** assigned to the third compound. The MMX calculated $^3J_{H,H}$ coupling constant between H(4B) and H(5) for structure **3** is 6.3 Hz while the observed value is 3.9 Hz. In this range of the Karplus-type relationship[18] a change in the dihedral angle exerts the greatest effect on the magnitude of the coupling constant. This may explain the differences between the observed and the calculated values for structure **3**. The relatively large change in coupling constant values can also be seen when comparing the calculated dihedral angle of 111° for **1** and 137° for **2**, which gives the corresponding coupling constant values of 3.1 and 7.5 Hz, respectively. All other calculated vicinal coupling constants for structure **3** are very close to the observed values and thus support the structure assignment.

Table 7. ^{17}O Chemical shifts in ppm for **1–3** (ext. D_2O).

Moiety	1	2	3
C=O	339.9	343.4	347
–O–	201.2	188.4	198
O(7)[a]	49.5	49.3	34
O(8)[a]	15.5	7.8	2

[a]Assignment is ambiguous.

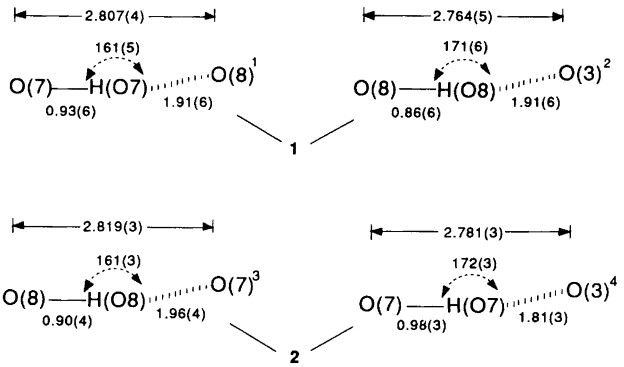

Symmetry codes: 1, *x*, 0.5−*y*, 0.5+*z*; 2, 0.5−*x*, −*y*, 0.5+*z*; 3, *x*−1, *y*, *z*; 4, *x*−1, *y*−1, *z*

Fig. 3. Hydrogen bonds (° and Å) and intermolecular O···O distances (Å) for **1** and **2**.

Table 8. Bond distances (Å) and angles (°) for **1** and **2** with e.s.d.s in parentheses.

	1	**2**		**1**	**2**
O(2)–C(1)	1.459(5)	1.440(3)	C(4)–H(4A)	1.08(5)	0.95(3)
O(2)–C(3)	1.340(6)	1.328(4)	C(4)–H(4B)	1.06(6)	0.97(3)
O(3)–C(3)	1.213(6)	1.207(3)	C(5)–C(6)	1.540(6)	1.524(4)
O(7)–C(7)	1.444(5)	1.449(3)	C(5)–H(5)	0.98(6)	0.93(3)
O(7)–H(O7)	0.93(6)	0.98(3)	C(6)–C(7)	1.533(6)	1.518(4)
O(8)–C(8)	1.440(5)	1.437(3)	C(6)–H(6A)	0.86(6)	0.99(4)
O(8)–H(O8)	0.86(6)	0.90(4)	C(6)–H(6B)	1.08(6)	1.05(3)
C(1)–C(5)	1.543(7)	1.547(5)	C(7)–C(8)	1.525(7)	1.525(4)
C(1)–C(8)	1.512(6)	1.516(4)	C(7)–C(9)	1.524(6)	1.508(4)
C(1)–H(1)	1.12(6)	0.98(3)	C(8)–H(8)	1.10(6)	1.04(3)
C(3)–C(4)	1.493(7)	1.475(5)	C(9)–H(9A)	0.99(6)	0.98(3)
C(4)–C(5)	1.535(6)	1.516(4)	C(9)–H(9B)	0.99(6)	1.04(3)
O(7)–C(3)	2.851(6)	—	C(9)–H(9C)	0.93(6)	1.00(3)
O(8)–C(3)	—	3.265(4)			
C(1)–O(2)–C(3)	110.8(3)	117.2(2)			
C(7)–O(7)–H(O7)	109(3)	111(2)	C(5)–C(6)–H(6A)	117(4)	115(2)
C(8)–O(8)–H(O8)	108(4)	102(2)	C(5)–C(6)–H(6B)	106(3)	111(2)
O(2)–C(1)–C(5)	106.9(3)	107.0(2)	C(7)–C(6)–H(6A)	102(4)	109(2)
O(2)–C(1)–C(8)	109.4(3)	113.2(2)	C(7)–C(6)–H(6B)	109(3)	106(2)
O(2)–C(1)–H(1)	103(3)	107(2)	O(7)–C(7)–C(6)	104.8(4)	106.0(2)
C(5)–C(1)–C(8)	107.1(4)	106.1(2)			
C(5)–C(1)–H(1)	120(3)	113(2)	O(7)–C(7)–C(8)	107.7(4)	106.1(3)
C(8)–C(1)–H(1)	110(3)	110(2)	O(7)–C(7)–C(9)	109.8(4)	109.7(3)
O(2)–C(3)–O(3)	119.6(4)	120.4(4)	C(6)–C(7)–C(8)	103.4(4)	103.4(2)
O(2)–C(3)–C(4)	111.8(3)	111.1(3)	C(6)–C(7)–C(9)	114.7(4)	115.5(3)
O(3)–C(3)–C(4)	128.3(4)	128.4(3)	C(8)–C(7)–C(9)	115.8(4)	115.2(3)
C03)–C(4)–C(5)	104.6(4)	106.6(3)	O(8)–C(8)–C(1)	108.8(4)	110.5(2)
C(3)–C(4)–H(4A)	112(3)	104(2)	O(8)–C(8)–C(7)	108.0(3)	106.6(2)
C(3)–C(4)–H(4B)	113(3)	107(2)	O(8)–C(8)–H(8)	111(3)	115(2)
C(5)–C(4)–H(4A)	114(3)	119(2)	C(1)–C(8)–C(7)	104.1(4)	102.1(2)
C(5)–C(4)–H(4B)	109(3)	110(2)	C(1)–C(8)–H(8)	112(3)	111(2)
H(4B)–C(4)–H(4A)	104(4)	109(3)	C(7)–C(8)–H(8)	113(3)	110(2)
C(1)–C(5)–C(4)	104.0(4)	102.8(2)	C(7)–C(9)–H(9A)	109(3)	108(2)
C(1)–C(5)–C(6)	105.5(4)	105.5(2)	C(7)–C(9)–H(9B)	114(3)	109(2)
C(4)–C(5)–C(6)	114.7(3)	117.2(2)	C(7)–C(9)–H(9C)	108(4)	113(2)
C(1)–C(5)–H(5)	112(3)	108(2)	H(9B)–C(9)–H(9C)	99(5)	105(3)
C(4)–C(5)–H(5)	108(3)	110(2)	H(9B)–C(9)–H(9A)	112(5)	114(3)
C(6)–C(5)–H(5)	112(3)	112(2)	H(9C)–C(9)–H(9A)	115(5)	109(3)
C(5)–C(6)–C(7)	104.4(4)	104.8(2)	O(7)–C(3)–O(3)	111.4(3)	—
H(6B)–C(6)–H(6A)	118(5)	111(3)	O(8)–C(3)–O(3)	—	127.6(2)

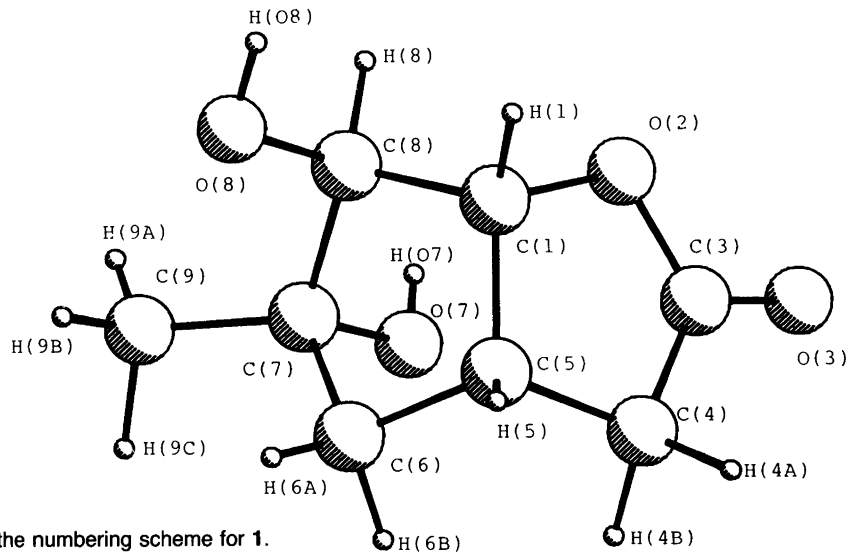

Fig. 4. PLUTO plot and the numbering scheme for **1**.

Table 9. Selected dihedral angles[a] (°) for **1** and **2** with e.s.d.s in parentheses.

Angle	1	2
O(2)–C(1)–C(5)–C(4)	6.7(4)	7.6(3)
O(2)–C(1)–C(5)–C(6)	−114.3(4)	131.0(2)
O(2)–C(1)–C(8)–O(8)	−155.3(4)	−36.0(3)
O(2)–C(1)–C(8)–C(7)	89.7(4)	−149.2(2)
O(2)–C(3)–C(4)–C(5)	13.8(5)	5.9(4)
O(3)–C(3)–C(4)–C(5)	−171.7(5)	−172.6(3)
O(7)–C(7)–C(8)–O(8)	172.8(3)	175.3(2)
O(7)–C(7)–C(8)–C(1)	−71.7(4)	−68.8(3)
C(1)–O(2)–C(3)–O(3)	175.1(4)	177.8(3)
C(1)–O(2)–C(3)–C(4)	−9.8(5)	−0.9(4)
C(1)–C(5)–C(6)–C(7)	21.0(4)	16.7(3)
C(3)–O(2)–C(1)–C(5)	1.6(5)	−4.5(3)
C(3)–O(2)–C(1)–C(8)	−114.1(4)	112.0(3)
C(3)–C(4)–C(5)–C(1)	−11.7(5)	−8.0(3)
C(3)–C(4)–C(5)–C(6)	102.9(4)	−123.2(3)
C(4)–C(5)–C(6)–C(7)	−92.8(4)	130.4(3)
C(5)–C(1)–C(8)–O(8)	89.1(4)	81.0(3)
C(5)–C(1)–C(8)–C(7)	−25.8(4)	−32.1(3)
C(5)–C(6)–C(7)–O(7)	75.7(4)	74.5(3)
C(5)–C(6)–C(7)–C(8)	−37.0(4)	−36.9(3)
C(5)–C(6)–C(7)–C(9)	−163.9(4)	−163.7(3)
C(6)–C(7)–C(8)–O(8)	−76.6(4)	−73.3(3)
C(6)–C(7)–C(8)–C(1)	38.9(4)	42.6(3)
C(8)–C(1)–C(5)–C(4)	123.9(4)	−113.6(3)
C(8)–C(1)–C(5)–C(6)	2.9(4)	9.8(3)
C(9)–C(7)–C(8)–O(8)	49.6(5)	53.7(3)
C(9)–C(7)–C(8)–C(1)	165.1(4)	169.6(3)

[a]For H–C–C–H angles see Table 6.

Bond distances and angles and torsion angles for **1** and **2** are presented in Tables 8 and 9. A view of the molecules **1** and **2** with numbering schemes are presented in Figs. 4 and 5. Stereoscopic packing views for **1** and **2** are shown in Figs. 6 and 7, respectively.

The structures of **1** and **2** show an intramolecular interaction between the *endo* oxygen and the carbonyl carbon. This type of incipient nucleophilic attack at the electrophilic carbon atom is defined[7] as O····C=O interaction and

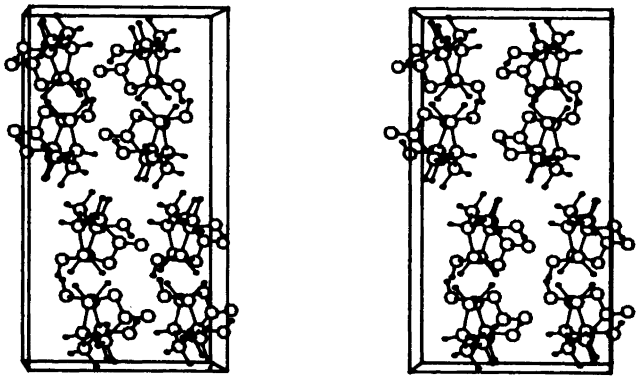

Fig. 6. Stereoscopic PLUTO plot for **1**. The *a* axis is vertical and *b* axis horizontal.

occurs readily when sterically possible. This type of interaction has been observed in other similar 2-oxa-*cis*-bicyclo[3.3.0]octan-3-one derivatives[2–6] with a small out-of-plane deformation of the carbonyl carbon towards the nucleophilic oxygen. In lactone **1** the intramolecular O····C distance, *d*, is 2.851(6) Å and the angle O····C=O, α, 111.4(3)°. These are very close to the optimum values for the strong O····C=O interaction.[7] The strong interaction in lactone **1** is also supported by the quite large out-of-plane deformation of the carbonyl carbon [C(3)] towards the *endo* oxygen [O(8)], the deformation, Δ, being 0.036(5) Å. This is by far the strongest intramolecular O····C=O interaction observed for 2-oxa-*cis*-bicyclo[3.3.0]octan-3-one derivatives. The *exo* conformation of the bicyclic lactone skeleton in lactone **2** (Table 9) makes it sterically unfavourable for a strong O····C=O interaction to occur. The negligible interaction is manifested by the long intramolecular O····C distance [d = 3.265(4) Å] and large O····C=O angle [α = 127.6°] together with small out-of-plane deformation [Δ = 0.010(3) Å].

Although the spatial arrangement of the cyclopentane ring substituents is different in lactones **1** and **2**, the hydro-

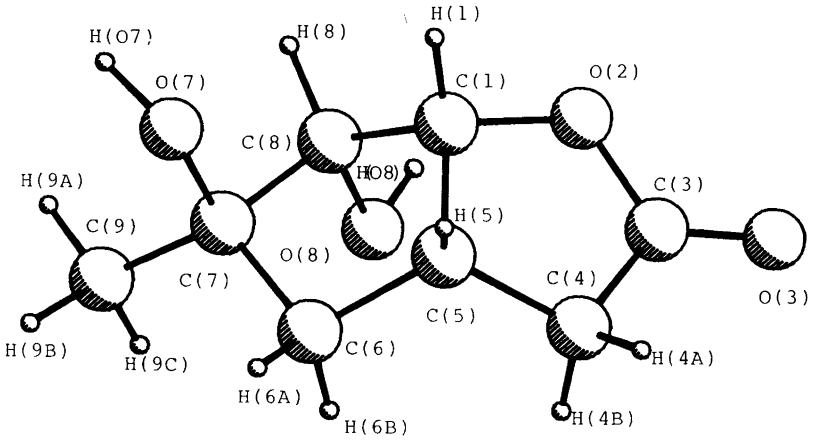

Fig. 5. PLUTO plot and the numbering scheme for **2**.

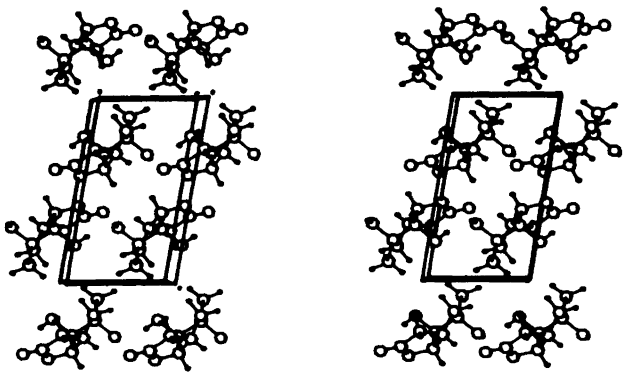

Fig. 7. Stereoscopic PLUTO plot for **2**. The *c* axis is vertical and *b* axis horizontal.

gen bonding and intermolecular O····O distances (Fig. 3) are very similar. The hydrogen bonding forms a similar pattern for both **1** and **2**. The *endo* hydroxy hydrogen [H(O7) in **1** and H(O8) in **2**] forms a hydrogen bond to the *exo* oxygen [O(8) in **1** and O(7) in **2**] of the adjacent molecule and, in addition, the *exo* hydrogen [H(O8) in **1** and H(O7) in **2**] is hydrogen bonded to the carbonyl oxygen [O(3)] of one more adjacent molecule. The intermolecular O····O distances and the O–H····O angles also show a similar exceptional pattern (Fig. 3).

The packing in the crystalline state (Figs. 6 and 7) is maintained by the exceptional hydrogen bonding in lactones **1** and **2**. This type of hydrogen bonding and formation of a crystal lattice may be hindered in the case of lactone **3** where the both hydroxy groups are situated on the same side of the cyclopentane ring (*endo,endo*). The absence of proper hydrogen bonding in lactone **3** may explain the failure to grow crystals good enough for an X-ray diffraction study.

In conclusion, the results obtained from ^{1}H NMR spectroscopy, X-ray diffraction and molecular mechanics calculations suggest that the bicyclic lactone skeleton remains structurally very similar in both solution and crystalline states. According to the molecular mechanics calculations, the bicyclic lactone moiety is rather flexible, but the energy differences between conformers are not remarkable. Therefore molecular mechanics calculations can indicate structures slightly different from those obtained from experimental X-ray and NMR data, as in the case of lactone **3**.

Acknowledgements. The authors thank Associate Professor Jouko Korppi-Tommola for permission to use the computer program PCMODEL (Serena Software). Financial support from the Finnish Academy in the form of research fellowship to K. R. is gratefully acknowledged.

References

1. Krow, G. R. *Tetrahedron 37* (1981) 2697.
2. Ferrier, R. J., Prasit, P. and Gainsford, G. J. *J. Chem. Soc., Perkin Trans 1* (1983) 1629.
3. Goldstein, S., Vannes, P., Houge, C., Frisque-Hesbain, A. M., Wiaux-Zamar, C., Ghosez, L., Germain, G., Declercq, J. P., Van Meerssache, M. and Arrieta, J. M. *J. Am. Chem. Soc. 103* (1981) 4616.
4. Stamos, I. K., Howie, G. A., Manni, P. E., Haws, W. J., Byrn, S. R. and Cassady, J. M. *J. Org. Chem. 42* (1977) 1703.
5. Murray-Rust, P. and Murray-Rust, J. *Acta Crystallogr., Sect. B 35* (1979) 1918.
6. Brown, A., Glen, R., Murray-Rust, P. and Murray-Rust, J. *J. Chem. Soc., Chem. Commun.* (1979) 1178.
7. Bürgi, H. B., Dunitz, J. D. and Shefter, E. *Acta Crystallogr., Sect. B 30* (1974) 1517.
8. Masar, S. E. and Krieger, H. *Suom. Kemistil. B 42* (1969) 1.
9. Masar, S. E. and Krieger, H. *Suom. Kemistil. B 43* (1970) 315.
10. Paasivirta, J. and Äyräs, P. *Suom. Kemistil. B 42* (1969) 379.
11. Walker, N. and Stuart, D. *Acta Crystallogr., Sect. A 39* (1983) 158.
12. Main, P., Fiske, S. J., Hull, S. E., Lessinger, L., Germain, G., Declercq, G. P. and Woolfson, M. M. MULTAN11/82, *System of Computer Programs for Automatic Solution of Crystal Structures,* Universities of York and Louvain, 1982.
13. Frenz, B. A. In: Schenk, H., Olthof-Hazekamp, R., van Kongsveld, H. and Bassi, G. C., Eds., The Enraf-Nonius CAD-4 SDP, *A Real-Time System for Concurrent X-Ray Data Collection and Crystal Structure Solution.* Computing in Crystallography, Delft University Press, Delft 1978, 64.
14. *International Tables for X-Ray Crystallography,* Kynoch Press, Birmingham, 1974, vol. IV.
15. Motherwell, W. D. S. and Clegg, W. PLUTO78, University of Cambridge, UK 1978.
16. Laatikainen, R. *J. Magn. Reson. 27* (1977) 169.
17. PCMODEL (version 2.0) is a 300-atom version of C. Still's (Columbia University) MODEL program (VAX version 1.1) modified by K. Steliou (University of Montreal) and for IBM-PC (or compatible) by M. M. Midland. Molecular mechanics (MMX) of PCMODEL is based on N. L. Allinger's program MM2(85), *QCPE* (1985).
18. Haasnoot, C. A. G., de Leeuw, F. A. A. M. and Altona, C. *Tetrahedron 36* (1979) 2783.

Received October 16, 1990.